Geomechanics and Engineering, *Vol. 43, No. 2 (2025) 75-87*
https://doi.org/10.12989/gae.2025.43.2.075

Influence of hemp geotextile to shear strength of soils

Eren Bayrakcı*[1], Eren Balaban[2], Mehmet İnanç Onur[2], Yücel Güney[3] and Yekta Karaduman[4]

[1]*Vocational School of Transportation, Eskişehir Technical University, Eskişehir, Turkey*
[2]*Faculty of Engineering, Department of Civil Engineering, Eskişehir Technical University, Eskisehir, Turkey*
[3]*School for the Handicapped, Anadolu University, Eskişehir, Turkey*
[4]*Department of Materials and Energy, Hemp Research Institute, Yozgat Bozok University, 66100, Yozgat, Turkey*

(*Received April 4, 2025, Revised September 10, 2025, Accepted October 10, 2025*)

Abstract. Natural geotextiles have been increasing instead of synthetic geotextiles used in various geotechnical engineering applications because they are more environmentally friendly. In this study, a new type of geotextile called "Geo-Hemptex" is produced from hemp fibers for the first time that may be an alternative to synthetic and natural geotextiles. Unconsolidated-Undrained (UU) and interface shear box tests were conducted to determine the interaction between Geo-Hemptex and granular soil. Geo-Hemptex was placed in one and two layers during UU tests, and three different confining pressures were applied during tests. Interface shear box tests were conducted under three different normal stresses to determine the interface characteristics between Geo-Hemptex and granular soil. All tests were also carried out using synthetic woven and non-woven geotextiles to compare with Geo-Hemptex. UU tests were modelled using the finite element method. All geotextiles provided approximately similar results in interface shear strength. However, higher adhesion was determined for Geo-Hemptex compared to synthetic woven geotextile. Geotextile placement, axial stiffness of geotextile, and interface strength influenced the UU test results. The synthetic woven geotextile yielded higher strength in the case of single-layer orientation. In contrast, Geo-Hemptex and woven synthetic geotextiles resulted in similar strength increases in the case of double layer orientation. The results of this study demonstrate that Geo-Hemptex can be used as an alternative to synthetic geotextiles, reducing greenhouse gas emissions and synthetic residues in the soil, thus providing more environmentally friendly solutions to geotechnical engineering problems.

Keywords: geotextile; hemp; reinforcement; shear strength; triaxial test

1. Introduction

Geotextiles are used in highway embankments, railway infrastructure, retaining walls, foundations, slope stability, and earth dams because geotextiles improve the shear strength of soils. Researchers carry out experimental studies to determine the effect of geotextiles on the shear strength of soils. Several studies in the literature have employed direct shear testing to assess both the shear strength and the interface shear strength (Mahmoodi *et al.* 2024, Son and Byun 2023, Ok *et al.* 2023, Dinarvand and Ardakani 2022, Arvin *et al.* 2021, Markou 2018, Jotisankasa and Rurgchaisri 2018, Toufigh *et al.* 2016, Vieira *et al.* 2015, Sayeed *et al.* 2014, Vieira *et al.* 2013, Subaida *et al.* 2008, Wasti and Özdüzgün 2001). In addition to that, triaxial tests were conducted using geotextiles inside the soil sample (Pradhan and Pothal 2024, Kantesaria and Sachan 2021, Talamkhani and Naeini 2021, Rezvani 2020, Jayawardane *et al.* 2020, Çiçek 2019, Shamsi *et al.* 2019, Nouri *et al.* 2016, Vashi *et al.* 2013, Latha and Murthy 2007). Finite element analysis was carried out for reinforced soils can be found in the literature for triaxial and shear box tests. (Skuodis *et al.* 2020, Lankaran *et al.* 2022, Hegde and Roy 2017, Cicek 2020, Xiangjing and Jianqing 2010, Roy *et al.* 2019) Those studies compared the results of FEM analysis with laboratory tests.

Geotextiles are generally produced from petroleum based synthetic fibers such as polypropylene, polyester, polyamide, and polyethylene. Therefore, geotextile production from synthetic fibers raises environmental concerns. Researchers are conducting studies to produce geotextiles from animal feathers or vegetable-based natural fibers. Cotton, flax, hemp, sisal, jute, kenaf, and coir fibers are the most commonly used fibers in the literature. Hemp fibers have higher tensile strength than other cellulosic fibers, increasing their strength when wet. Hemp fibers are durable against salty water, alkaline, chemicals, and microorganisms. Hemp fibers also resist UV lights (Karakaya 2021, Mangut and Karahan 2011, Gedik *et al.* 2010, Peev 2012).

Hemp fibers have gained interest in civil engineering applications due to their high strength. Several studies have used hemp fibers to produce environmentally friendly construction materials. These studies utilized hemp fibers to produce bio-composites, insulation materials, concrete mixtures, new types of bricks, asphalt mixtures and cement (Akdere 2023, Shewalul *et al.* 2023, Bennai *et al.* 2022, Guo *et al.* 2020, Hamzaoui *et al.* 2020, Aslan 2020, Serin *et al.* 2018, Balčiūnas *et al.* 2017, Pundiene *et al.* 2022, Kremensas *et al.* 2018, Mungkung *et al.* 2018, Kallakas *et al.* 2018, Murphy *et al.* 2010). Hemp fiber is even used to strengthen reinforced concrete elements in the laboratory due to their high strength (Ghalieh *et al.* 2017). Standard

*Corresponding author, Assistant Professor
E-mail: erenbayrakci@eskisehir.edu.tr

ISSN: 2005-307X (Print), 2092-6219 (Online)

Table 1 Granular soil's physical and mechanical properties

Parameter	Value
Specific Gravity	2.71
Gravel (%)	6.2
Sand (%)	82.1
Silt (%)	10.2
Clay (%)	1.5
Coefficient of Uniformity, C_u	43.14
Coefficient of Curvature, C_c	3.21
Liquid Limit, LL	NP
Plastic Limit, PL	NP
Plasticity Index, PI	NP
Optimum Water Content (%)	4
Maximum Dry Unit Weight, (gr/cm^3)	2.17
Maximum Void Ratio, e_{max}	0.635
Minimum Void Ratio, e_{min}	0.282
Soil Classification	SP

Table 2 Material properties of Geo-Hemptex

Thickness (mm)	Mass per Unit Area (g/m^2)	Tensile Strength (kN/m)		Elongation at Break (%)		Static Puncture Load (CBR) (kN)	Dynamic Puncture Resistance (mm)
		XMD	MD	XMD	MD		
1.55	424	33.74	33.75	8.7	16.5	4.06	8.32

geotechnical engineering laboratory tests were carried out to determine the effect of hemp fibers on the shear strength parameters of soils (Ammar *et al.* 2019, El Ahmad *et al.* 2019, Diab *et al.* 2016, Najjar *et al.* 2014). Ouagne *et al.* (2017) investigated the potential use of hemp fibers to produce geotextiles. However, to the authors, no research has been done on hemp fibers' geotextile production. This study presents the first production of woven geotextile from hemp fibers. The effect of the produced woven hemp geotextile (Geo-Hemptex) on the shear strength parameters of granular soil was evaluated, and the interface strength between the geotextile and granular soil was determined. Additionally, triaxial tests were modeled using the finite element method.

2. Material and method

2.1 Material

A local firm provided the granular soil used in this study. The physical properties of the granular soil were determined. Sieve analysis was carried out according to ASTM D6913-17, hydrometer analysis was carried out according to ASTM D7928-21e1, and specific gravity was determined according to ASTM D854-14. Granular soil was classified according to the unified soil classification system (ASTM D2487-11). Minimum and maximum void ratios were determined according to ASTM D4253-16 and ASTM D4254-16 respectively. The proctor test determined the maximum dry unit weight and optimum water content

Fig. 1 Geo-Hemptex

(ASTM D698-12). Table 1 summarizes the physical and mechanical properties of the granular soil.

Woven Geo-Hemptex was produced using commercially available hemp yarns provided by Kingdom Hemp Company, China. Woven Geo-Hemptex fabrics were weaved using hemp yarns with a yarn count of Nm 9.6 (104 tex). Firstly, five of these yarns were folded together to obtain coarser yarns that are more suitable for geotextile production. For this purpose, five Nm 9.6 yarns were folded together to get a resulting yarn count of Nm 1.92 (≈520 tex). These coarse yarns were used as warp and weft yarns to produce plain-weave geotextiles called Geo-Hemptex. Plain (1/1) weave type was chosen in this study since it is the most preferred weave type in the industry. Plain weaving also provides the highest tensile strength when compared with other weaving types. Warp and weft density of the Geo-Hemptex fabrics were 6 and 4 yarns/cm, respectively.

Mass per unit area, maximum tensile strength and corresponding elongation at warp direction and weft direction, static puncture test and dynamic puncture test

Table 3 Material properties of PP geotextiles

Geotextile Type	Mass per Unit Area (g/m^2)	Tensile Strength in warp and weft direction (kN/m)	Elongation at Failure (%)	Static Puncture Load (CBR) (kN)	Dynamic Puncture Resistance (mm)
Woven	308	33/33	3	9	7
Nonwoven	525	34/34	≥ 50	6.3	3

were carried out according to TS EN ISO 9863-1, TS EN ISO 9864, TS EN ISO 10319, TS EN ISO 12236, and TS EN ISO 13433, respectively. Each test was repeated five times to demonstrate the repeatability and reliability of the results. All tensile tests were carried out using specimens of 20 cm x 20 cm dimensions. The difference between results was less than 10% for each test. The average results of these tests are provided in Table 2.

Geo-Hemptex was developed as an environmentally friendly alternative to synthetic geotextiles used in industry. Therefore, this study also uses polypropylene (PP) woven and non-woven geotextiles, and test results are compared with those of Geo-Hemptex. The material properties of the PP geotextiles used in this study are given in Table 3.

2.2 Methods

Unconsolidated undrained triaxial tests (UU) were carried out to determine the effect of Geo-Hemptex on the shear strength parameters of the soil. Interface shear box tests were also conducted to determine the interface shear parameters between granular soil. All tests were also carried out for synthetic geotextiles to compare Geo-Hemptex and Synthetic geotextiles. Soil samples were prepared at 50% relative density so that the effect of geotextile reinforcements could be better observed, as Goodarzi and Shahnazari (2019) suggested.

2.2.1 Shear box and interface shear box tests

The shear strength parameters of the soil were determined by a shear box test per ASTM D3080/3080M-23. A shear box with dimensions of 10*10 cm was used throughout the study. 50% relative density is achieved after soil placement. Granular soil is placed by compaction method. Soil is compacted in three layers to the shear box. A great care is taken so that, shearing plane and compaction layer interface do not coincide. The shear box tests were conducted under 50 kPa, 100 kPa, and 150 kPa vertical stresses. The shear rate was chosen as 0.20 mm/min. The shear box test ended when the shear displacement reached 10 mm. Each shear box test was repeated three times to show repeatability. The results presented in this study are average values of those tests.

Interface shear box tests were carried out according to ASTM D5321-21. Interface shear test samples are prepared by compacting granular soil in three layers. Interface shear box tests were also repeated three times to show the repeatability of the results. As described by Afzali-Nejad *et al.* (2017), samples were prepared and shown in Fig. 2. A metal plate was placed in the lower half of the shear box to prevent the geotextile from bending. The geotextile was also secured with tape to ensure it did not deform in the

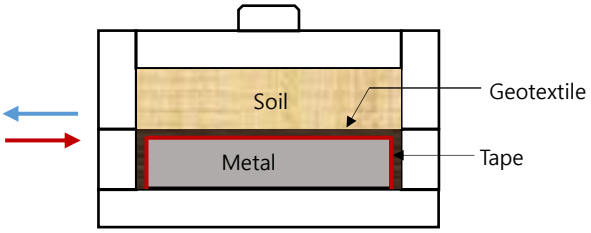

Fig. 2 Modified shear box assembly

shearing direction. Double side tape is used to attach geotextile to metal box for interface shear tests. Bottom part of the tape is glued to metal box, while geotextile is glued to upper section of the tape. All geotextiles are cut 12 cm in length and 10 cm in width which allowed taping geotextile to side walls of metal plate. This assembles methodology made it possible to measure shear forces developed between granular soil and geotextile. The soil with 50% relative density was placed in the upper half of the shear box.

Interface shear box tests were also carried out under 50 kPa, 100 kPa, and 150 kPa vertical stresses, which are generally used in the literature (Razeghi and Ensani 2023, Vieira *et al.* 2013, Lopes and Silvano 2010, Punetha *et al*. 2017, Stacho *et al*. 2023). The shear rate was chosen as 0.25 mm/min following the methodology used by Markou (2018). The interface shear box test ended when horizontal displacement reached 10%. The friction and adhesion interface angle between soil and geotextile were determined between soil and Geo-Hemptex, PP woven geotextile, and PP non-woven geotextile.

2.2.2 Triaxial tests

The UU tests were carried out according to ASTM D2850-23 to determine the shear strength of granular soil and the contribution of geotextile reinforcements to the shear strength of soil. ELE Digital Tritest 50 Load frame machine was used to carry out UU tests. UU soil samples were prepared using the wet tamping method described by Gürbüz and Afacan (2022) at a relative density of 50%. The samples were 70 mm in diameter and 140 mm in height. Vacuum is applied to granular soil samples so that the sample can maintain its integrity until cell pressure is applied. 25 kPa, 50 kPa, and 100 kPa cell pressures were applied during the UU tests. The axial loading rate was chosen as 0.9 mm/min. Load and displacement values were recorded at every 0.1% axial deformation up to 0.5% of axial deformation. Afterwards, data were recorded at every 0.25% axial deformation. UU tests were ended when axial deformation reached 15%. Geotextile reinforcements were placed inside the sample, as shown in Fig. 3.

The UU test results showed the contribution of Geo-Hemptex to shear strength and shear strength parameters of

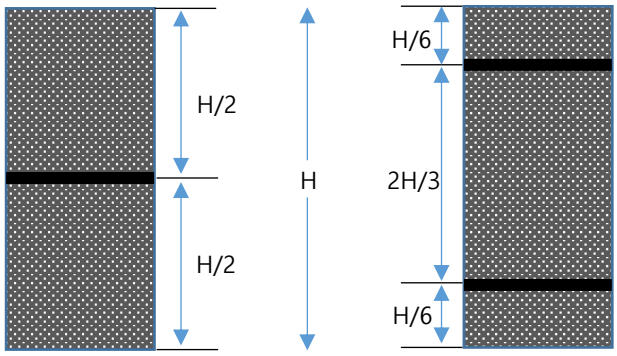

Fig. 3 Geotextile placement inside the soil samples

Table 4 Abbreviations used for UU samples

Sample Type	Abbreviation
Geo-Hemptex Single Layer	GH1
Geo-Hemptex Double Layer	GH2
PP Woven Geotextile Single Layer	PP/W1
PP Woven Geotextile Double Layer	PP/W2
PP Non-Woven Geotextile Single Layer	PP/NW1
PP Non-Woven Geotextile Double Layer	PP/NW2

granular soil. The contribution of Geo-Hemptex was compared with those of PP-woven and PP non-woven geotextiles.

Table 4 shows abbreviations used for the samples tested under UU conditions.

2.2.3 Numerical method

The UU triaxial tests were modelled using the finite element method using Plaxis 2D v23.2 software. The deviator stresses, shear strength parameters, and failure planes obtained from the experimental study were compared with the results of the finite element method. Therefore, the effects of geotextiles on failure mechanisms were explored.

Finite element models were created using axisymmetry to comply with the experimental study. The hardening soil model was used to model granular soil. Geogrid element was used for the geotextiles. The axial stiffness parameters were obtained from tensile tests carried out in the scope of this study. The Axial stiffness of Geo-Hemptex, PP woven, and PP non-woven geotextiles were determined as 388 kN/m, 1100 kN/m, and 68 kN/m, respectively. Boundary conditions were defined to be the same as those in the experimental study. Deviator stresses measured during tests were applied in the axial direction in the finite element model. If the soil sample did not fail under the applied deviator stresses, the deviator stress was gradually increased until the soil sample failed. Axial stress distribution was investigated at a cross-section where maximum shear stresses were calculated. The average of those axial stresses was compared with deviator stresses measured during the experimental study.

3. Results and discussion

3.1 Interface Shear Box Test Results

This study initially conducted shear box tests, and the shear stress-deformation curves are provided in Figure 4. The soil's friction angle and cohesion were 39.7^0 and 7.76 kPa, respectively.

The shear stress-deformation curves between granular soil and different geotextiles are given in Fig. 5.

When shear stress–deformation curves are examined, the highest shear stress is observed at the PP/NW-sand interface. This indicates that the PP/NW geotextile provided the highest interface shear strength. The shear stresses at the GH-sand interface are close to those at the PP/W–sand interface. Tanchaisawat *et al*. (2010) stated that the efficiency of geosynthetic reinforcement should be determined by friction resistance and adhesion. Eqs. (1) and (2) are used to assess friction resistance and adhesion efficiency.

$$E_c = \left(\frac{c_a}{c}\right).100(\%) \quad (1)$$

$$E_\phi = \left(\frac{tan\delta}{tan\phi}\right).100(\%) \quad (2)$$

Ec represents adhesion efficiency, Eϕ represents friction efficiency in equations. c, ca, ϕ (º) and δ (º) stand for cohesion, adhesion, angle of friction and interface friction angle respectively. Interaction coefficient is also defined to compare the soil's shear strength with the interface shear strength between the soil and the geotextile (Gruchot *et al*. 2020). The interaction coefficient can be calculated according to Eq. (3) below.

$$R_i = \frac{\tau_{fa}}{\tau_f} = \frac{\sigma_n.tan\delta + c_a}{\sigma_n.tan\phi + c} \quad (3)$$

τ_f, τ_{fa} and σ_n represents soil's shear strength, interface shear strength and normal stress respectively.

Table 5 summarizes shear box test results of sand and interface strength between sand and different geotextiles.

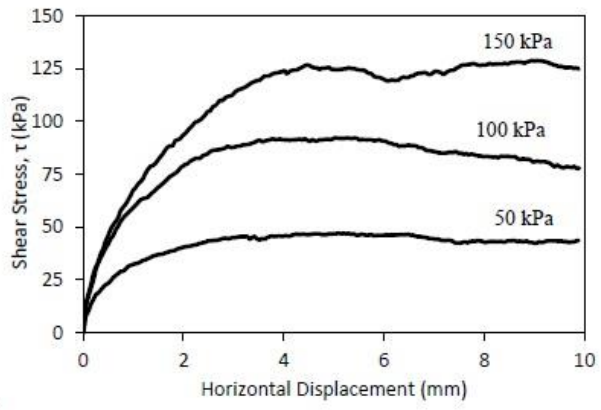

Fig. 4 Granular soil shear stress-deformation curves

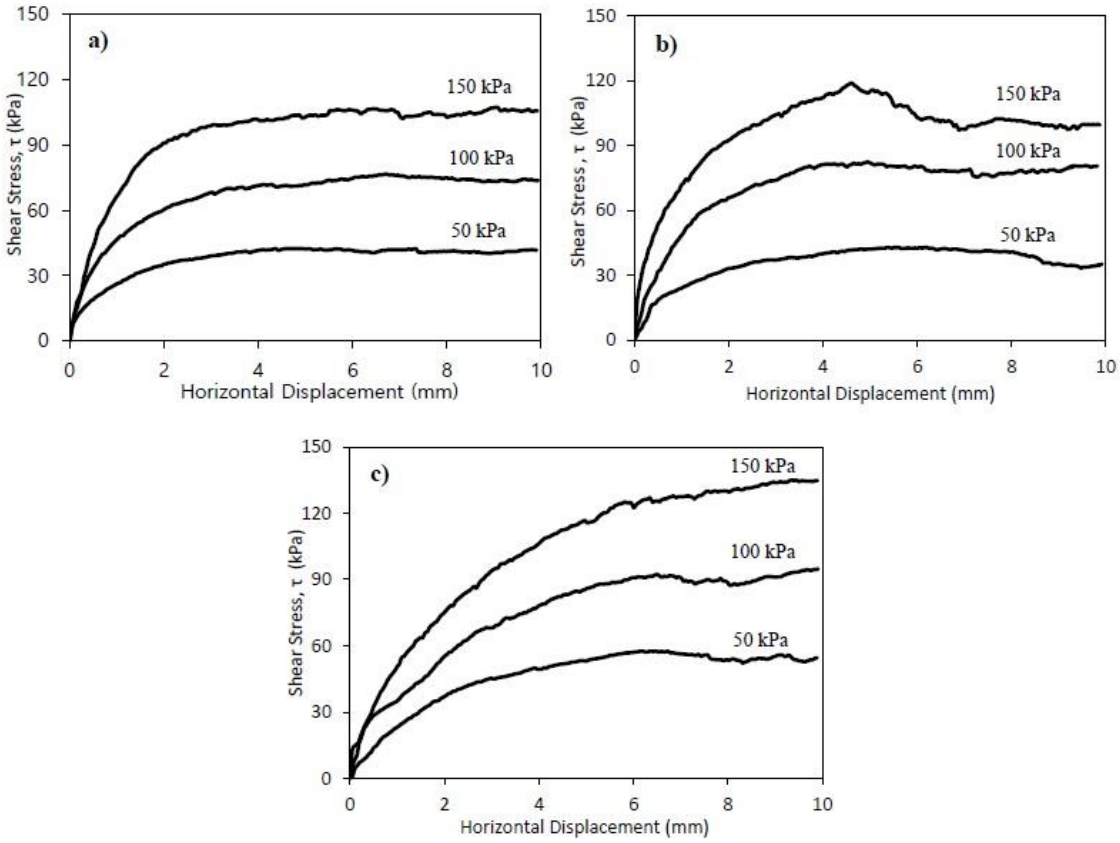

Fig. 5 Interface shear stress-deformation curves (a) GH-sand (b) PP/W-sand and (c) PP/NW-sand

Table 5 Shear box test results for sand and sand-geotextile interfaces

Sand		GH – Sand			PP/W – Sand			PP/NW – Sand		
c (kPa)	**ϕ (º)**	**c_a (kPa)**		**δ (º)**	**c_a (kPa)**		**δ (º)**	**c_a (kPa)**		**δ (º)**
7.76	39.7	8.66		34.6	5.43		37.7	18.45		38.2
		E_c (%)		**E_ϕ (%)**	**E_c (%)**		**E_ϕ (%)**	**E_c (%)**		**E_ϕ (%)**
		111.6		83.1	70.0		93.1	237.8		94.8
		R_i			**R_i**			**R_i**		
		50 (kPa)	**100 (kPa)**	**150 (kPa)**	**50 (kPa)**	**100 (kPa)**	**150 (kPa)**	**50 (kPa)**	**100 (kPa)**	**150 (kPa)**
		0.88	0.86	0.85	0.89	0.91	0.92	1.18	1.07	1.03

When Table 5 is examined, it is seen that adhesion provided by GH is higher than that of PP/W. Even though GH-sand's interface strength equals PP/W-sand, different adhesion can be explained by the various surface textures of geotextiles. In addition, the highest interface measured for the PP/NW-sand interface can also be explained by the texture properties of the PP/NW geotextile. Interface strength is higher if the surface of the geotextile is rough and the geotextile has wider openings, as stated by Markou (2018) and Sayeed *et al*. (2014). Fig. 6 shows X32 zoomed microscope images of the geotextiles used in this study. It is clear from Fig. 6 that the PP/NW geotextile has the roughest surface, followed by GH. GH has also has wider openings and rougher surface than PP/W. Therefore, adhesion values are found the highest for PP/NW and followed by GH and PP/W respectively. Wider openings on the geotextiles cause soil particles to fill them, which results in limited lateral movement of soil particles—interlocking soil particles to opening results in higher adhesive forces between soil and geotextile. Pictures given in Fig. 6 prove the above explanations.

3.2 UU test results

Deviator stress–axial strain curve of sand is given in Fig. 7. The angle of friction and cohesion of granular soil are determined as 43.62^0 and 9 kPa, respectively.

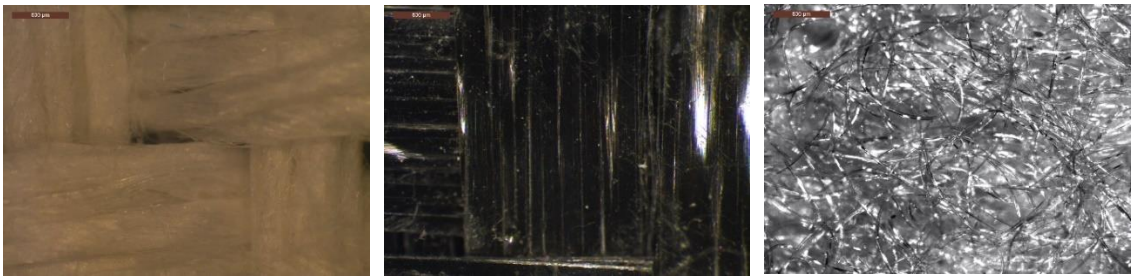

(a) (b) (c)

Fig. 6 Microscopic views of geotextiles (X32) (a) GH, (b) PP/W and (c) PP/NW

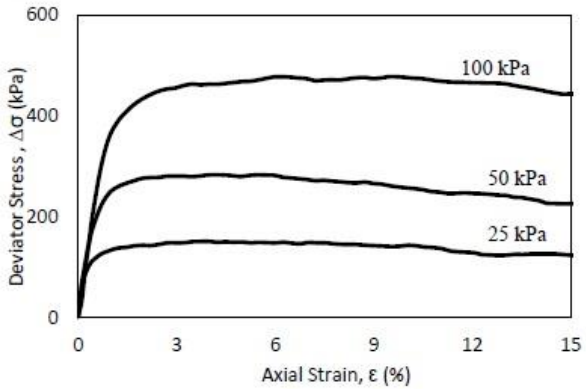

Fig. 7 Deviator stress-axial strain curve of sand determined from UU tests

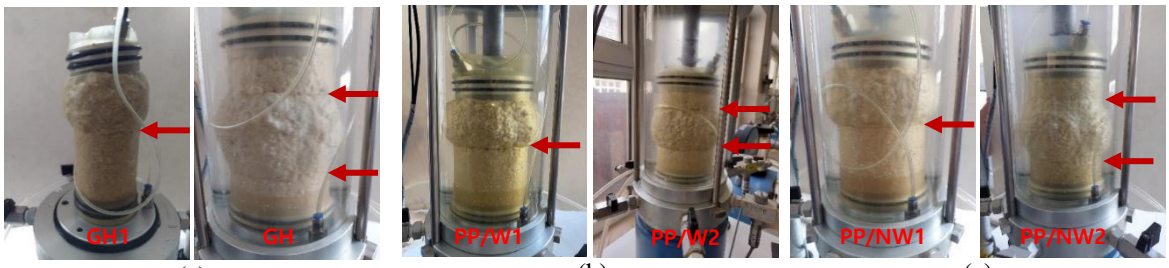

(a) (b) (c)

Fig. 8 Geotextile reinforced sand samples after UU tests (a) GH1 – GH2, (b) PP/W1- PP/W2 and (c) PP/NW1 – PP/NW2

Soil samples reinforced with geotextile after UU tests are given in Fig. 8.

The failure pattern of sand samples resembles the studies of Goodarzi and Shahnazari (2019) and Haeri *et al.* (2000). Failure is observed at the upper part of the sample in the case of a single layer geotextile for each geotextile. Geotextiles divided the sample into two parts and changed failure behaviour. Failure is observed at the upper part before the geotextile transfers load to the lower part due to samples being prepared at medium relative density. Geotextiles increased rigidity at lower and upper parts in case of double layer placement. Friction forces between geotextile reinforcements and soil restricted lateral deformation of soil sample. This yielded lateral deformation between two geotextiles and changed failure behaviour. Failure modes influenced soil samples aspect ratio in the case of single and double-layer reinforcement cases. The decreasing aspect ratio also increased soil samples' shear strength and geotextile reinforcement. Stress-axial deformation curves are given in Fig. 9.

In the case of single-layer reinforcement, PP/W1 experiences the highest strength increase, followed by PP/NW1 and GH1. This behaviour is due to geotextiles' axial stiffness and their interface strength with sand. Goodarzi and Shahnazari (2019) also state that geotextile axial stiffness positively affects strength increase. However, the influence of interface strength on the sample's failure mechanism is also known.

The higher strength increase in the case of PP/NW than GH because PP/NW-sand interface strength is higher in the case of single layer placement. Therefore, the PP/NW geotextile restricts the lateral deformation of sand more than GH. When test results of single-layer reinforcement are investigated in the case of single-layer orientation, the highest deviator stress is measured for PP/W1. Deviator stresses increased around 100% compared to sand for 25, 50, and 100 kPa cell pressure. PP/NW1 resulted in a 75%

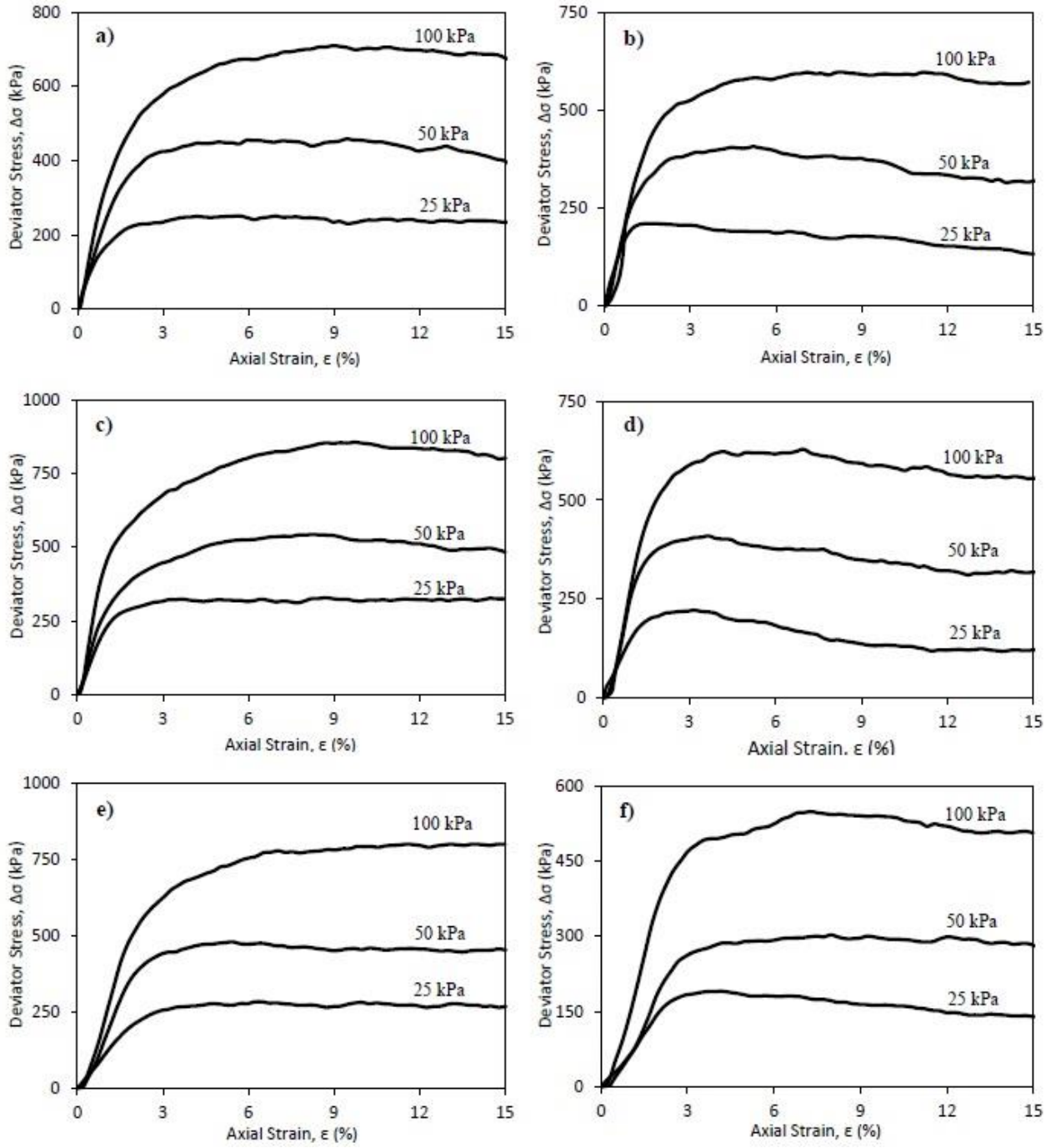

Fig. 9 UU tests with geotextile reinforcements (a) GH1, (b) GH2, (c) PP/W1, (d) PP/W2, (e) PP/NW1 and (f) PP/NW2

deviator stress increase; in the case of GH1 samples, it increased 60% deviator stress.

The highest strength increase is observed for PP/W2, followed by GH2 and PP/NW2 in the case of double-layer reinforcement. GH resulted in a higher strength increase than PP/NW in the case of double-layer reinforcement. This change can be explained by the higher axial stiffness of GH than PP/NW. Interface strength between geotextile and sand resulted in lateral deformation of the sample between geotextile layers, which failed the sample. Geotextile with a higher axial stiffness resulted in a higher strength increase.

Deviator stress increased approximately 41% compared with sand samples in the PP/W2 geotextile case for 25, 50, and 100 kPa cell pressure. In the case of GH2 reinforcement, deviator stress increase equals 37%. The lowest strength increment is measured for PP/NW2 samples as 16%.

A two-layer reinforcement arrangement resulted in lower strength than a single-layer reinforcement. The same conclusion is reached by Goodarzi and Shahnazari (2019), Haeri *et al.* (2000), and Koerner (2005). Therefore, the location of reinforcement is as important as several

geotextile layers. Goodarzi and Shahnazari (2019) stated that geosynthetic reinforcement should be placed at a higher lateral deformation section. Haeri *et al.* (2000) explained that geotextile layers should be placed where maximum tensile deformations are observed. Higher strength improvements can be measured for the same geotextile layer number instead of randomly placed geotextile layers. Koerner (2005) also stated that geotextile layers placed at upper and lower parts of samples do not contribute to the shear strength of samples. Those places are defined as ineffective zones. It is also stated that reinforcement benefits can be better observed when geotextiles are placed at the center of the sample or 1/3 of the sample if two layers of geotextiles are used. From those explanations, it is understood that geotextile reinforcements are beneficial when placed where the failure plane passes through.

Geotextile reinforcements increased the ductility of UU samples. Higher axial deformation is observed in samples with geotextile reinforcements at low axial deformations due to the compressibility of geotextiles. In addition, restriction of lateral deformation and prevention of failure plane progress by geotextile reinforcements also increases the ductility of tested UU samples. The highest ductility is observed when PP/NW geotextiles are placed inside soil samples since PP/NW geotextile is the thickest and has the lowest axial stiffness.

3.3 Finite element modelling of UU tests

This section provides the results of the finite element modelling of UU tests. Fig. 10 shows the shear deformations of soil samples with one and two-layer geotextile reinforcements.

Two shear planes are observed in the case of single-layer reinforcement. The first shear plane starts from the bottom left of the sample and ends at the right bottom side of the reinforcement. The second shear plane starts from the top right side of the reinforcement and ends with the left upper side of the sample. Geotextile reinforcement acts as a symmetry axis. Three different shear planes are observed when two geotextile reinforcements are placed inside the sample. The first failure plane is observed from the top left of the soil sample to the top right of reinforcement.

Failure planes are observed between two geotextile reinforcements. The last failure plane extends from the right bottom of the geotextile to the left bottom of the sample. Failure deformations cover a larger area between the two reinforcements, indicating higher deformation at this part. More significant deformations were observed during the UU tests in this section.

Deviator stress distribution may be seen in Fig. 11. It can be seen that deviator stresses in single-layer geotextile reinforcement concentrate at the outer part of the sample and the symmetry axis. Deviator stress decreases where failure planes pass through. The decrease of deviator stress is thought to be due to deformations caused by failure planes. Several geotextile layers influence deviator stress distribution. Deviator stresses are higher between two geotextiles when double-layer reinforcement is provided inside the sample. For both geotextile placement patterns, lower deviator stresses are calculated around the geotextile

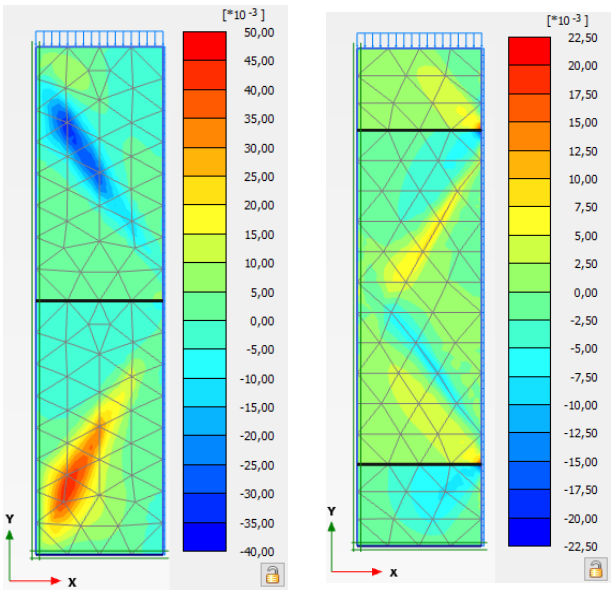

(a) (b)

Fig. 10 Shear deformations obtained from finite element modelling (a) one layer reinforcement and (b) two layers reinforcement

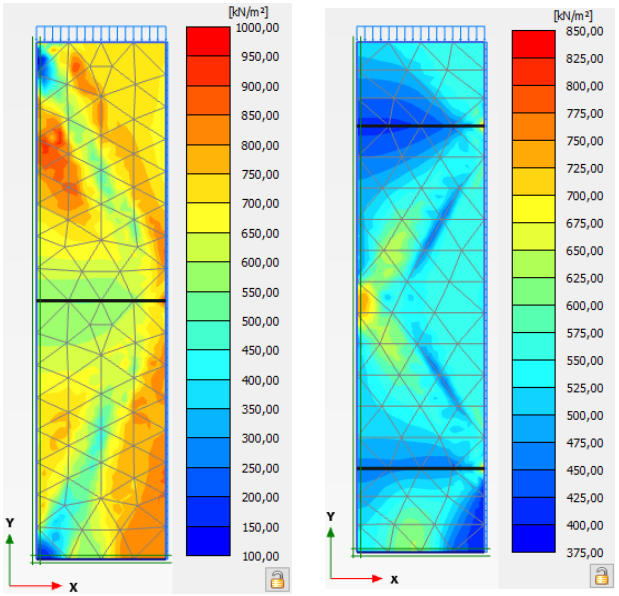

(a) (b)

Fig. 11 Deviator stress distribution inside the samples (a) single layer reinforcement and (b) double layer reinforcement

layers. However, deviator stress increases at the edges of the geotextile. This could be due to friction forces developed at the sand-geotextile interface. Since interface friction forces decrease at the edges, higher deviator stress increases at the edge of the sample. Lateral deformations of samples for single and double-layer reinforcement arrangements are given in Fig. 12. The geotextile layer number changes the lateral deformation behaviour of samples.

Lateral deformations are concentrated on the sample's top right and bottom right when a single-layer geotextile is

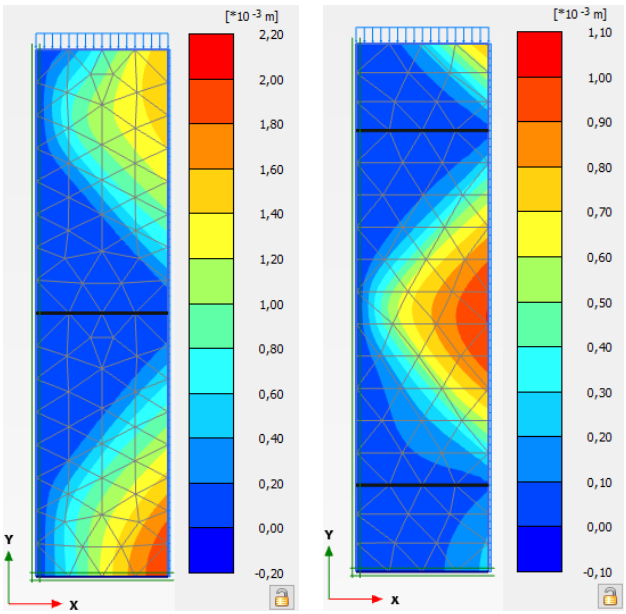

(a) (b)

Fig. 12 Lateral deformations calculated after finite element analysis (a) single layer reinforcement and (b) double layer reinforcement arrangement

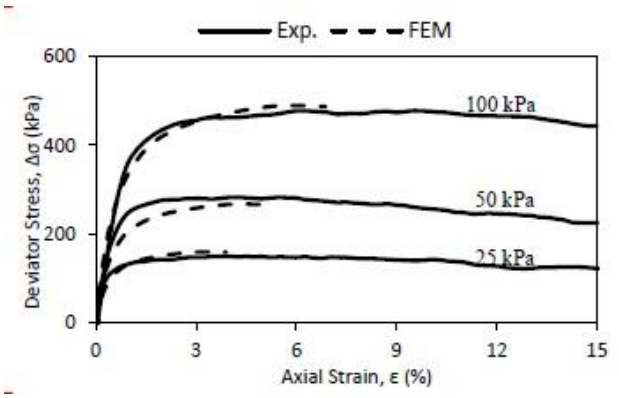

Fig. 13 Deviator stress-axial deformation of sand obtained from laboratory tests and finite element analysis

placed in the middle of the soil. However, swelling is observed at the top half of the sample at the laboratory tests, as seen in Figure 8. Lateral deformations calculated using the finite element method comply with experimental observations of double geotextile arrangements. Lateral deformations are concentrated between two geotextile layers both at laboratory and finite element method (FEM). Geotextiles were placed at the top and bottom of the sample, and rigidity increased at those places.

Deviator stress-axial deformation curves are compared from laboratory tests and finite element analysis. Deviator stress–axial deformation curves for sand are given in Fig. 13, while geotextile reinforced samples deviator stress-axial deformation curves are given in Fig. 14. When stress-deformation curves are investigated, curves obtained from finite element analysis end at lower deformation levels. As cell pressure increases, finite element analysis calculates higher strains. This behaviour is per the study of Lankaran *et al*. (2022).

Table 6 UU test results and Finite element method results

Sample Type	c (kPa)	ϕ (°)	Deviator Stress (kPa)		
			25 kPa	50 kPa	100 kPa
Sand	9	43.62	150.40	282.80	477.50
Sand-FEM	6	44.20	160.31	267.90	489.70
GH1	22	48.60	251.30	458.40	709.60
GH1-FEM	23	48.17	276.70	450.17	713.80
PP/W1	28	51.24	328.10	543.40	856.70
PP/W1-FEM	27	50.85	338.50	551.53	862.27
PP/NW1	22	50.00	282.30	478.40	798.40
PP/NW1-FEM	22	49.83	286.22	491.95	790.77
GH2	21	45.41	211.50	408.50	598.80
GH2-FEM	20	46.39	232.81	419.40	638.14
PP/W2	20	46.71	221.90	409.60	628.50
PP/W2-FEM	19	47.18	236.41	421.43	637.23
PP/NW2	17	44.13	190.40	302.70	548.60
PP/NW2-FEM	16	44.57	206.43	317.59	544.61

When stress-deformation curves are compared, finite element analysis correctly models soil behaviour. Although there is deviation at the plastic parts of the curves, there is less than a 10% difference in peak deviator stresses between laboratory tests and finite element analysis. Skuodis *et al.* (2020) observed similar behaviour. Pure sand samples can be more correctly modelled in stress-deformation curves' elastic and plastic parts.

All UU test results and finite element analysis results are summarized on Table 6.

Stress-Deformation curves obtained from FEM differs from test result at the elastic part of the curve while, differences between curves reduce at the plastic part of the curve when PP/NW reinforcement is used. Since the compressibility of PP/NW geotextile cannot be modelled correctly in finite element analysis, compressibility causes higher deformations, which resulted in deviation at the elastic part of the stress-deformation curve.

Similar stress-deformation curves are obtained from FEM and UU tests when GH is used. However, the difference between stress-deformation curves increases when double layer of GH is used.

PP/W reinforcements can also be modelled similarly to UU test results. However, the stress-deformation behaviour differs from test results at higher cell pressures, and a double-layer reinforcement layer was used. In this case, a higher elasticity modulus is calculated than from the UU test results.

It is possible to say that; FEM results comply with laboratory test results in general. Even though there are differences in modelling stress-deformation curves, the highest deviator stresses obtained from FEM are consistent with test results.

4. Conclusions

In this study Geo-Hemptex is produced (for the first time) and its effect on the shear strength of sand is investigated.

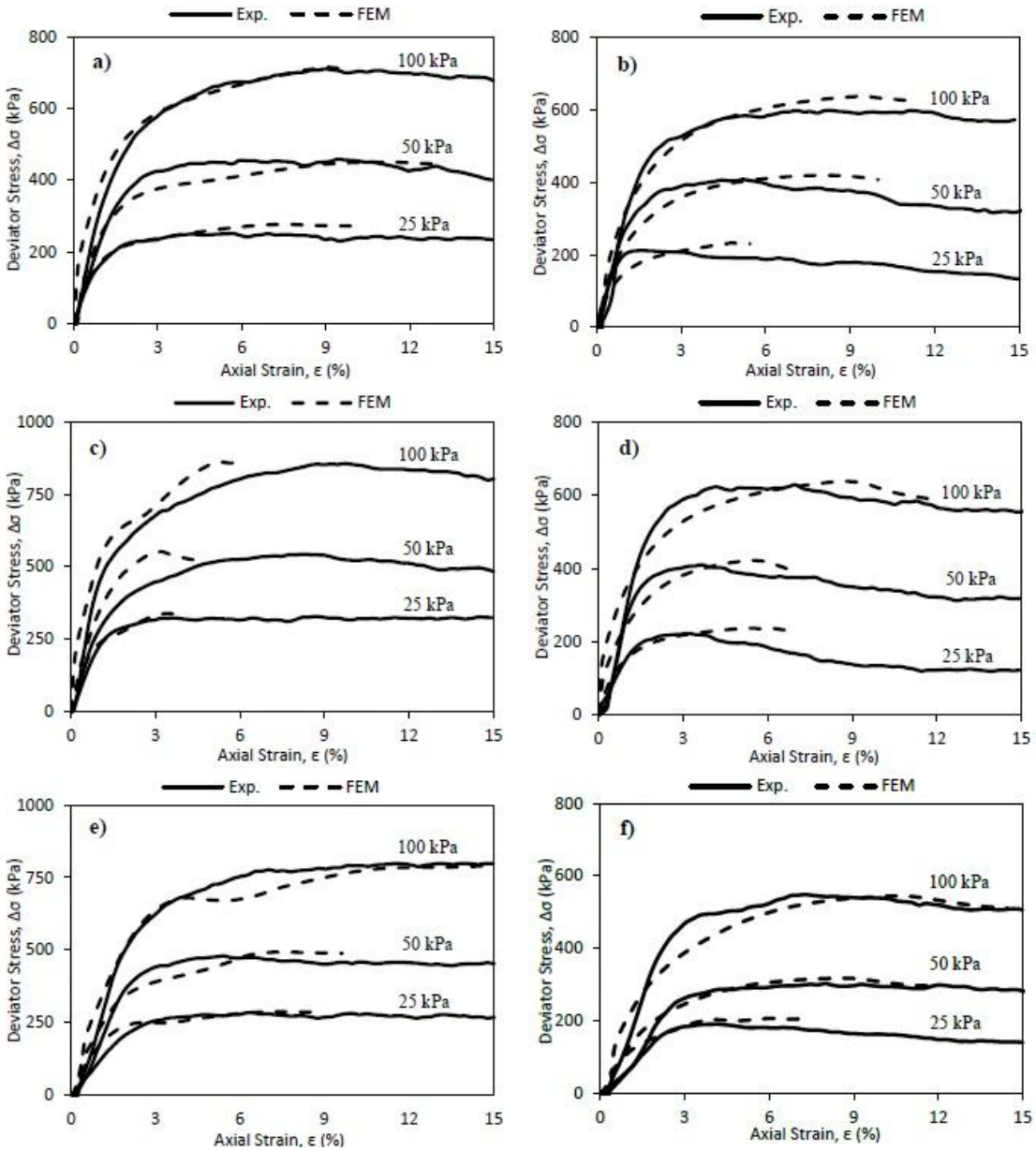

Fig. 14 UU tests and finite element analysis deviator stress-axial strain comparison (a) GH1, (b) GH2, (c) PP/W1, (d) PP/W2, (e) PP/NW1 and (f) PP/NW2

Triaxial UU tests and shear box tests were performed to determine the impact of Geo-Hemptex on the shear strength of sand. All tests were repeated for synthetic polypropylene geotextiles used in the construction sector. Therefore, the results obtained for Geo-Hemptex could be compared with those of its artificial counterparts. UU triaxial tests were also modelled using the finite element method. Differences between test results and finite element analysis are also revealed. The results of this study are summarized below.

- Geo-Hemptex provided a similar interface shear strength to sand PP/W. However, due to its surface texture properties, the GH-sand interface has higher adhesion to sand.
- The highest strength increase is measured for PP/W, followed by PP/NW and GH, in a single-layer geotextile. In a double-layer arrangement, the highest strength increase is measured for PP/W, followed by GH and PP/NW geotextile.
- Maximum deviator stresses obtained from PP/W and GH are close to each other in case of a double-layer arrangement.
- Geotextile's axial stiffness and interface strength with sand affect triaxial test results.
- Failure is observed at the part of the sample in the case of a layer geotextile, while failure is observed between two geotextiles in the case of a double-layer arrangement.
- The strength of the sample with a double-layer geotextile arrangement is lower than the single-layer geotextile layer in this study.
- Geotextile reinforcement increases the ductility of soil samples. Due to their compressibility, geotextiles

increase axial deformations. Geotextiles also constrain lateral deformations of soil samples and, to some degree, prevent a failure plane from developing inside the soil sample.

- The finite element analysis results comply with the UU test results. When maximum deviator stress is considered, the difference between laboratory test results and finite element analysis is less than 10%. Finite element analysis can produce approximately the same stress-deformation curves as laboratory test results.

The study concluded that Geo-Hemptex's have the potential to become a new, environmentally friendly product for use in the industry, based on experimental and numerical analysis results. Geo-Hemptex which produced for the first time for this study provided results which are comparable with its synthetic counterparts. With the increasing importance of environmental friendliness and sustainability globally, geotextiles made from natural fibers, along with synthetic geotextiles, have begun to gain a foothold in the industry. Geo-Hemptex is produced from totally natural fibers which makes it a good alternative for the construction industry. Production of Geo-Hemptex will damage environment less when compared with synthetic geotextiles. In addition, since Geo-Hemptex is a natural product, it will not leave any by products on soil. According to results of this study, Geo-Hemptex can be used in temporarily constructed road embankments over soft soil in the real life applications if the service life of embankment is lower than the service life of Geo-Hemptex. Improving service life of Geo-Hemptex can be further studied in the future.

Acknowledgements

Eskisehir Technical University Scientific Research Project supported this work under project number 22DRP218. The authors express their gratitude for the support.

References

Afzali-Nejad, A., Lashkari, A. and Shourijeh, P.T. (2017), "Influence of particle shape on the shear strength and dilation of sand-woven geotextile interfaces", *Geotext. Geomembranes*, **45**(1), 54-66. https://doi.org/10.1016/j.geotexmem.2016.07.005.

Akdere, İ. (2023), "The usability of Hemp fiber in the production of foam concrete", Master's thesis, Afyon Kocatepe University, Afyon.

Ammar, A., Najjar, S.S. and Sadek, S. (2019), "Mechanics of the interface interaction between Hemp fibers and compacted clay", *Int. J. Geomech.*, **19**(4), 04019015. https://doi.org/10.1061/(ASCE)GM.1943-5622.0001368.

Arvin, M.R., Ghafary, G.R., Hataf, N. and Ghafary, A.R. (2021), "Shear behavior of EPS geofoam reinforced with polypropylene fiber", *Geomech. Eng.*, **25**(5), 347-355. https://doi.org/10.12989/gae.2021.25.2.347.

Aslan, İ. (2020), "Investigation of usability of natural Hemp fiber instead of cellulosic fiber in stone mastic asphalt", Master's thesis, Yozgat Bozok University, Yozgat.

ASTM D698 – 12 (2021), Standard Test Methods for Laboratory Compaction Characteristics of Soil Using Standard Effort (12,400 ft-lbf/ft3 (600 kN-m/m3)). ASTM International, West Conshohocken, PA.

ASTM D854 – 14 (2016), Standard Test Methods for Specific Gravity of Soil Solids by Water Pycnometer. ASTM International, West Conshohocken, PA.

ASTM D2487 – 11 (2020), Standard Practice for Classification of Soils for Engineering Purposes (Unified Soil Classification System). ASTM International, West Conshohocken, PA.

ASTM D2850 – 23 (2023), Standard Test Method for Unconsolidated-Undrained Triaxial Compression Test on Cohesive Soils. ASTM International, West Conshohocken, PA.

ASTM D3080/3080M-23 (2023), Standard Test Method for Direct Shear Test of Soils Under Consolidated Drained Conditions. ASTM International, West Conshohocken, PA.

ASTM D4253 – 16 (2019), Standard Test Methods for Maximum Index Density and Unit Weight of Soils Using a Vibratory Table. ASTM International, West Conshohocken, PA.

ASTM D4254 – 16 (2016), Standard Test Methods For Minimum Index Density And Unit Weight Of Soils And Calculation Of Relative Density. ASTM International, West Conshohocken, PA.

ASTM D5321 – 21 (2021), Standard Test Method for Determining the Shear Strength of Soil-Geosynthetic and Geosynthetic-Geosynthetic Interfaces by Direct Shear. ASTM International, West Conshohocken, PA.

ASTM D6913 – 17 (2017), Standard Test Methods for Particle-Size Distribution (Gradation) of Soils Using Sieve Analysis. ASTM International, West Conshohocken, PA.

ASTM D7928-21e1 (2021), Standard Test Method for Particle-Size Distribution (Gradation) of Fine-Grained Soils Using the Sedimentation (Hydrometer) Analysis. ASTM International, West Conshohocken, PA.

Balčiūnas, G., Kizinievič, V. and Gargasas, J. (2017), "Physical properties of building blocks from hemp shives aggregate and cementitious binder, manufactured in the expanded clay (Vibro Pressing) production line", *Materials Science Forum*, **908**, 118-122. https://doi.org/10.4028/www.scientific.net/MSF.908.118.

Bennai, F., Ferroukhi, M.Y., Benmahiddine, F., Belarbi, R. and Nouviaire, A. (2022), "Assessment of hygrothermal performance of hemp concrete compared to conventional building materials at overall building scale", *Constr. Build. Mater.*, **316**. https://doi.org/10.1016/j.conbuildmat.2021.126007.

Cicek, E. (2020), "Experimental and theoretical investigation for highways incorporating geotextile design methodology", *Road Mater. Pavement Design*, **21**(4), 965-984. https://doi.org/10.1080/14680629.2018.1532314.

Cicek, E. (2019), "The effects of different types of fibres and geotextiles for pavement design", *Road Mater. Pavement Design*, **20**(4), 793-814. https://doi.org/10.1080/14680629.2017.1417890.

Diab, A.A., Sadek, S., Najjar, S. and Daya, M.H.A. (2016), "Undrained shear strength characteristics of compacted clay reinforced with natural Hemp fibers", *Int. J. Geotech. Eng.*, **10**(3), 263-270. https://doi.org/10.1080/19386362.2015.1132122.

Dinarvand, R. and Ardakani, A. (2022), "Shear behavior of geotextile-encased gravel columns in silty sand-experimental and SVM modeling", *Geomech. Eng.*, **28**(5), 505-520. https://doi.org/10.12989/gae.2022.28.5.505.

El Ahmad, M.E., Sadek, S. and Najjar, S. (2019), "Drained triaxial response of clay reinforced with natural hemp fibers", *Proceedings of the 8th International Conference on Case Histories in Geotechnical Engineering*, VA: American Society of Civil Engineers, 305-314. https://doi.org/10.1061/9780784482117.031.

Gedik, G., Avinç, O.O. and Yavaş, A. (2010), "Hemp fiber properties and its advantages in textile industry", *Electron. J. Text. Technol.*, **4**(3), 39-48.

Ghalieh, L., Awwad, E., Saad, G., Khatib, H. and Mabsout, M. (2017), "Concrete columns wrapped with hemp fiber reinforced polymer–

an experimental study", *Procedia Eng.*, **200**, 440-447. https://doi.org/10.1016/j.proeng.2017.07.062.

Goodarzi, S. and Shahnazari, H. (2019), "Strength enhancement of geotextile-reinforced carbonate sand", *Geotext. Geomembranes*, **47**(2), 128-139. https://doi.org/10.1016/j.geotexmem.2018.12.004.

Gruchot, A., Zydroń, T. and Michalska, A. (2020), "The influence of compaction and water conditions on shear strength and friction resistance between geotextiles and ash-slag mixture", *Energies*, **13**(5), 1086. https://doi.org/10.3390/en13051086.

Guo, A., Sun, Z., Qi, C. and Sathitsuksanoh, N. (2020), "Hydration of portland cement pastes containing untreated and treated hemp powders", *J. Mater. Civil Eng.*, **32**(6). https://doi.org/10.1061/(asce)mt.1943-533.0003209.

Gürbüz, S. and Afacan, K. B. (2022), "Influence of silts on very loose clean sand's static liquefaction and dilative response", *Eskişehir Osmangazi University Engineering and Architecture Faculty*, **30**(2), 242-252. https://doi.org/10.31796/ ogummf.1073656.

Haeri, S.M., Noorzad, R. and Oskoorouchi, A.M. (2000), "Effect of geotextile reinforcement on the mechanical behavior of sand", *Geotext. Geomembranes*, **18**(6), 385-402. https://doi.org/10.1016/S0266-1144(00)00005-4.

Hamzaoui, R., Guessasma, S., Abahri, K. and Bouchenafa, O. (2020), "Formulation of modified cement mortars using optimal combination of fly ashes, shiv and hemp fibers", *J. Mater. Civil Eng.*, **32**. https://doi.org/10.1061/(ASCE)MT.1943-5533.0002918.

Hegde, A. and Roy, R. (2018), "A comparative numerical study on soil–geosynthetic interactions using large scale direct shear test and pullout test", *Int. J. Geosynth. Ground Eng.*, **4**(1), 2. https://doi.org/10.1007/s40891-017-0119-1.

Jayawardane, V.S., Anggraini, V., Li-Shen, A.T., Paul, S.C. and Nimbalkar, S. (2020), "Strength enhancement of geotextile-reinforced fly-ash-based geopolymer stabilized residual soil", *Int. J. Geosynth Ground Eng.*, **6**(4), 50. https://doi.org/10.1007/s40891-020-00233-y.

Jotisankasa, A. and Rurgchaisri, N. (2018), "Shear strength of interfaces between unsaturated soils and composite geotextile with polyester yarn reinforcement", *Geotext. Geomembranes*, **46**(3), 338-353. https://doi.org/10.1016/j.geotexmem.2017.12.003.

Kallakas, H., Närep, M., Närep, A., Poltimäe, T. and Kers, J. (2018), "Mechanical and physical properties of industrial hemp-based insulation materials", *Proceedings of the Estonian Academy of Sciences*, **67**(2), 183-192. https://doi.org/10.3176/proc.2018.2.10.

Kantesaria, N. and Sachan, A. (2021), "Undrained shear behaviour of fly ash-geosynthetic system with woven and non-woven geotextile", *Proceedings of the Indian Geotechnical Conference 2019: IGC-2019*, Springer Singapore. https://doi.org/10.1007/978-981-33-6466-0_14.

Karakaya, E. (2021), "Ecological pretreatment of Hemp fibers", Master's thesis, Erciyes University, Kayseri.

Koerner, R.M. (2005), *Designing with Geosynthetics,* 5th Ed., New Jersey, USA: Prentice Hall, 796p.

Kremensas, A., Kairytė, A., Vaitkus, S. and Vėjelis, S. (2018), "Physical-mechanical properties of composites from hemp shives and starch", *Int. J. Eng. Sci. Invent.*, **7**, 43-49.

Lankaran, Z.E., Nik Daud, N.N., Rostami, V. and Yusoff, Z.M. (2022), "Consolidated drained triaxial test on treated coastal soil and finite element analysis using PLAXIS 2D", *Adv. Mater. Sci. Eng.*, 15 pages. https://doi.org/10.1155/2022/7263333.

Latha, G.M. and Murthy, V.S. (2007), "Effects of reinforcement form on the behavior of geosynthetic reinforced sand", *Geotext. Geomembranes*, **25**(1), 23-32. https://doi.org/10.1016/j.geotexmem.2006.09.002.

Lopes, M.L. and Silvano, R. (2010), "Soil/geotextile interface behaviour in direct shear and pullout movements", *Geotech. Geol. Eng.*, **28**, 791-804. https://doi.org/10.1007/s10706-010-9339-z.

Mahmoodi, K., Motlagh, N.M. and Ardakani, A.R.M. (2024), "An investigation into the effects of lime-stabilization on soil-geosynthetic interface behavior", *Geomech. Eng.*, **38**(3), 231-247. https://doi.org/10.12989/gae.2024.38.3.231.

Mangut, M. and Karahan, N. (2011), *Textile Fibers*, 4th Ed., Bursa.

Markou, I.N. (2018), "A study on geotextile—sand interface behavior based on direct shear and triaxial compression tests", *Int. J. Geosynth. Ground Eng.*, **4**, 8. https://doi.org/10.1007/s40891-017-0121-7.

Mungkung, R., Intrachooto, S., Srisuwanpip, N., Lamai, A., Sorakon, K. and Kittipakornkarn, K. (2018), "Life cycle assessment of hempstone for green buildings", *Chem. Eng. Transact.*, **63**, 247-252. https://doi.org/10.3303/CET1863042.

Murphy, F., Pavia, S. and Walker, R. (2010), "An assessment of the physical properties of lime-hemp concrete", *Proceeding of the bridge and concrete research in Ireland*, Cork.

Najjar, S.S., Sadek, S. and Taha, H. (2014), "Use of hemp fibers in sustainable compacted clay systems", *Proceedings of the Geo-Congress 2014: Geo-characterization and Modeling for Sustainability*, Atlanta, 1415-1424. https://doi.org/10.1061/9780784413272.138.

Nouri, S., Nechnech, A., Lamri, B. and Lopes, M.L. (2016), "Triaxial test of drained sand reinforced with plastic layers", *Arabian J. Geosci.*, **9**, 1-9. https://doi.org/10.1007/s12517-015-2017-y.

Ok, B., Colakoglu, H. and Dagli, U. (2023), "Evaluation of the geogrid-various sustainable geomaterials interaction by direct shear tests", *Geomech. Eng.*, **34**(2), 173-186. https://doi.org/10.12989/gae.2023.34.2.173.

Ouagne, P., Renouard, S., Michel, D. and Laine, E. (2017), "Mechanical properties of flax and hemp yarns designed for the manufacturing of geotextiles. Improvement of the resistance to soil born microorganisms", *J. Textile Eng. Fashion Technol.*, **1**(5), 210-215. https://doi.org/10.15406/jteft.2017.01.00034.

Peev, P.I. (2012), "Is industrial hemp a sustainable construction material?", *Bachelor of Architectural Technology and Construction Management*, Denmark: Via University College, Horsens.

Pradhan, S.K. and Pothal, G.K. (2024), "Shear strength characteristics of pond ash reinforced with polymeric and natural fiber geosynthetic", *Geotech. Geol. Eng.*, **1**-22. https://doi.org/10.1007/s10706-024-02765-w.

Pundiene, I., Vitola, L., Pranckeviciene, J. and Bajare, D. (2022), "Hemp shive-based bio-composites bounded by potato starch binder: the roles of aggregate particle size and aspect ratio", *J. Ecol. Eng.*, **23**(2), 220-234. https://doi.org/10.12911/22998993/144637.

Punetha, P., Mohanty, P. and Samanta, M. (2017), "Microstructural investigation on mechanical behavior of soil - geosynthetic interface in direct shear test", *Geotext. Geomembranes*, **45**(3), 197-210. https://doi.org/10.1016/j.geotexmem. 2017.02.001

Razeghi, H.R. and Ensani, A. (2023), "Clayey sand soil interactions with geogrids and geotextiles using large-scale direct shear tests", *Int. J. Geosynth. Ground Eng.*, **9**(2), 24. https://doi.org/10.1007/s40891-023-00443-0.

Rezvani, R. (2020), "Shearing response of geotextile-reinforced calcareous soils using monotonic triaxial tests", *Mar. Georesour. Geotec.*, **38**(2), 238-249. https://doi.org/10.1080/1064119X.2019.1566936.

Roy, R., Venkateswarlu, H. and Hegde, A. (2019), "Numerical study on cyclic shear behavior of soil–geosynthetics interface.", In Geotechnics for Transportation Infrastructure: Recent Developments, Upcoming Technologies and New Concepts, **2**, 235-245. Singapore: Springer Singapore. https://doi.org/10.1007/978-981-13-6713-7_19.

Sayeed, M.M.A., Ramaiah, B.J. and Rawal, A. (2014), "Interface shear characteristics of jute/polypropylene hybrid nonwoven geotextiles and sand using large size direct shear test", *Geotext. Geomembranes*, **42**(1), 63-68. https://doi.org/10.1016/j.geotexmem.2013.12.001.

Serin, S., Macit, M.E., Çınar, E.C. and Çelik, S. (2018), "Effect of using natural Hemp fiber on asphalt concrete mixtures", *Düzce*

University Journal of Science and Technology, **6**(4), 732-744. https://doi.org/10.29130/dubited.428492.

Shamsi, M., Ghanbari, A. and Nazariafshar, J. (2019), "Behavior of sand columns reinforced by vertical geotextile encasement and horizontal geotextile layers", *Geomech. Eng*, **19**(4), 329-342. https://doi.org/10.12989/gae.2019.19.4.329.

Shewalul, Y. W., Quiroz, N.F., Streicher, D. and Walls, R. (2023), "Fire behavior of hemp blocks: A biomass-based construction material", *J. Build. Eng.*, 2352-7102. https://doi.org/10.1016/j.jobe.2023.108147.

Skuodis, Š., Dirgėlienė, N. and Medzvieckas, J. (2020), "Using triaxial tests to determine the shearing strength of geogrid-reinforced sand", *Studia Geotechnica et Mechanica*, **42**(4), 341-354. https://doi.org/10.2478/sgem-2020-0005.

Son, D.G. and Byun, Y.H. (2023), "Shear strength characteristics of two-layer geotextile reinforced with flowable fill", *Constr. Build. Mater.*, **367**, 130207. https://doi.org/10.1016/j.conbuildmat.2022.130207.

Stacho, J., Sulovska, M. and Slavik, I. (2023), "Analysis of the shear strength of a soil-geosynthetic interface", *Civil Environ. Eng.*, **19**(1), 452-463. https://doi.org/10.2478/cee-2023-0040.

Subaida, E.A., Chandrakaran, S. and Sankar, N. (2008), "Experimental investigations on tensile and pullout behaviour of woven coir geotextiles", *Geotext. Geomembranes*, **26**(5), 384-392. https://doi.org/10.1016/j.geotexmem.2008.02.005.

Talamkhani, S. and Naeini, S.A. (2021), "The undrained shear behavior of reinforced clayey sand", *Geotech. Geol. Eng.*, **39**, 265-283. https://doi.org/10.1007/s10706-020-01490-4.

Tanchaisawat, T., Bergado, D.T., Voottipruex, P. and Shehzad, K. (2010), "Interaction between geogrid reinforcement and tire chip–sand lightweight backfill", *Geotext. Geomembranes*, **28**(1), 119-127. https://doi.org/10.1016/j.geotexmem.2009.07.002.

Toufigh, V., Ouria, A., Desai, C.S., Javid, N., Toufigh, V. and Saadatmanesh, H. (2016), "Interface behavior between carbon-fiber polymer and sand", *J. Test. Eval.*, **44**(1), 385-390. https://doi.org/10.1520/JTE20140153.

TS EN ISO 9863-1 (2020), Geosynthetics - Determination of thickness at specified pressures - Part 1: Single layers, TSE.

TS EN ISO 9864 (2005), Geosynthetics - Test method for the determination of mass per unit area of geotextiles and geotextile-related products, TSE.

TS EN ISO 10319 (2015), Geosynthetics - Wide-width tensile test, TSE.

TS EN ISO 12236 (2007), Geosynthetics - Static puncture test (CBR test), TSE.

TS EN ISO 13433 (2008), Geosynthetics - Dynamic perforation test (cone drop test), TSE.

Vashi, M.J., Desai, A.K. and Solankib, C.H. (2013), "Behavior of geotextile reinforced flyash+ clay-mix by laboratory evaluation", *Geomech. Eng.*, **5**(1), 331-342. https://doi.org/10.12989/gae.2013.5.4.331.

Vieira, C.S., Lopes, M.D.L. and Caldeira, L. (2015), "Sand-Nonwoven geotextile interfaces shear strength by direct shear and simple shear tests", *Geomech. Eng.*, **9**(5), 601-618. https://doi.org/10.12989/gae.2015.9.5.601.

Vieira, C.S., Lopes, M.D.L. and Caldeira, L.M. (2013), "Sand-geotextile interface characterisation through monotonic and cyclic direct shear tests", *Geosynth. Int.*, **20**(1), 26-38. https://doi.org/10.1680/gein.12.00037.

Wasti, Y. and Özdüzgün, Z.B. (2001), "Geomembrane–geotextile interface shear properties as determined by inclined board and direct shear box tests", *Geotext. Geomembranes*, **19**(1), 45-57. https://doi.org/10.1016/S0266-1144(00)00002-9.

Xiangjing, H. and Jianqing, J. (2010), "Finite element analysis of triaxial tests of a new composite reinforced soil", *Proceedings of the 2010 International Conference on Intelligent Computation Technology and Automation*, IEEE. https://doi.org/10.1109/ICICTA.2010.67.

IC